Application of autoresonance in rapid beam extraction of synchrotrons

X. Ding,[1,2] S. Ruan,[1,2] H. Ren,[1] G. Wang,[1] R. H. Zhu,[1,2] J. C. Yang,[1,2,*] H. Zhao,[1,2,†] and G. D. Shen[1,2,‡]

[1]*Institute of Modern Physics, Chinese Academy of Sciences, Lanzhou 730000, China*
[2]*University of Chinese Academy of Sciences, Beijing 100049, China*

(Received 3 March 2025; accepted 11 September 2025; published 24 October 2025)

In recent years, ultrahigh dose rate (FLASH) radiotherapy has become a novel cancer treatment technique because of its similar tumor-killing efficacy as conventional particle therapy while significantly protecting normal tissues. However, due to the limitation of the number of particles, achieving FLASH condition in a compact heavy-ion synchrotron requires a short spill time of tens of milliseconds, which is challenging for the conventional rf-KO method. To tackle this challenge, we introduce autoresonance into the third-order resonant extraction for the first time, offering an alternative to the conventional approach of merely increasing the excitation amplitude. Resulting from a strong detuning effect, a frequency sweeping excitation with small amplitude can drive the entire beam into the autoresonant state, thus enabling rapid beam extraction within a single sweeping period. Compared with the conventional method, this innovative method requires only the addition of an octupole magnet. At the same time, conventional slow extraction rf-KO employs a repetitive multicycle frequency sweeping excitation, a specific particle resonates when the sweeping frequency aligns with its tune. In contrast to the autoresonance rf-KO, which engages the entire beam in resonance simultaneously. In this research, the autoresonance threshold of a particle in the presence of sextupole and octupole magnetic fields is analyzed, and the single particle simulation shows good agreement with the theoretical formula. Furthermore, the autoresonance-based rapid extraction process is simulated and studied, showing the possibility of millisecond scale beam extraction.

DOI: 10.1103/s85n-289k

I. INTRODUCTION

Particle accelerators play an important role in fundamental and applied research in the sciences, as well as in many technical and industrial fields. Among them, particle therapy has undergone impressive development in the past few decades, due to its excellent physical dose localization at the Bragg peak and a high biological effect, especially for heavy ion beams [1]. Since the first dedicated therapy facility was built in the 1990s, more than 150 particle therapy facilities are in operation and under construction by the end of 2024, and more than 410,000 patients have been treated worldwide [2]. In recent years, it has been demonstrated that ultrahigh dose rates (>40 Gy/s) provide significant normal cell sparing effects while maintaining an equivalent tumor response to conventional dose rates (0.001–0.4 Gy/s) [3,4]. This FLASH effect has great promise and is considered one of the most important discoveries in recent radiotherapy history.

FLASH irradiation using proton beam is relatively straightforward due to the high beam current from cyclotrons. However, it is challenging to achieve FLASH conditions on carbon ion therapy facilities, which usually use compact synchrotrons and provide much lower dose rates than cyclotrons. Considering the limitation of the number of particles in compact synchrotrons, a much shorter extraction duration is the most effective way to realize the ultrahigh dose rates. Typically, the spill time for FLASH therapy requires reducing proton/ion spill time in synchrotron from seconds to less than 100 ms, which is the so-called rapid extraction [5,6].

rf-knockout (rf-KO) method with frequency modulation and amplitude modulation is widely used in synchrotrons to drive the beam from the stable to the unstable region to achieve beam extraction, in which the modulation is mainly to cover the incoherent tunes due to various nonlinear effects [7–9]. Usually, the spill time of conventional rf-KO slow extraction is in the second scale, corresponding to the multiple excitation modulation cycles [10]. One way to speed up the extraction time to one or several modulation cycles is to increase the strength of the excitation. For example, the Heidelberg Ion-Beam Therapy Center (HIT)

*Contact author: yangjch@impcas.ac.cn
†Contact author: hezhao@impcas.ac.cn
‡Contact author: shenguodong@impcas.ac.cn

Published by the American Physical Society under the terms of the Creative Commons Attribution 4.0 International license. Further distribution of this work must maintain attribution to the author(s) and the published article's title, journal citation, and DOI.

achieved carbon beam extraction within approximately 150 ms by increasing the rf driver power to 50 times larger [1]. However, the high-voltage rf driver increases construction costs and introduces technical challenges.

In this article, we propose to introduce autoresonance into the rf-KO method, which will effectively reduce the power requirement of the driver and thus efficiently achieve rapid extraction in synchrotrons. Autoresonance is the natural tendency of a weakly driven nonlinear system to remain in resonance with its driver under certain conditions, even if the system parameters vary in time and/or space. It has been well studied in various dynamical systems such as atomic and molecular systems [11,12], plasma systems [13–15], fluids [16], and magnetics [17,18]. Recently, a comprehensive study has also been carried out for the first time in accelerator physics [19]. The autoresonance technique enables nonlinear oscillators to achieve large oscillation amplitudes by applying a swept frequency excitation, in which the beam decoherence effect is minimized and phase locking is maintained with the drive as long as the excitation amplitude is above a specific threshold. Theoretically, this threshold mainly depends on the detuning parameter of the machine and the frequency sweep rate of the driver. The conventional rf-KO extraction method has a large threshold due to the small detuning parameter, making it difficult to achieve the autoresonance condition and cannot excite all particles to a large amplitude at the same time. We propose to reduce the autoresonance threshold by intentionally introducing a strong detuning, and demonstrate that this can be achieved using octupoles while ensuring that the third-order resonance extraction process is not significantly affected. A comprehensive study is conducted on the autoresonance threshold in the presence of sextupole and octupole fields. The beam dynamics of the autoresonance and the resulting rapid extraction process are simulated, and the results are consistent with the analytical model.

This paper is organized as follows: Sec. II discusses the autoresonance threshold theory in the presence of sextupole and octupole fields, and presents a single particle simulation based on the slow extraction lattice of the SESRI synchrotron [9]. Section III discusses the differences between conventional slow extraction and autoresonance rapid extraction, followed by an analysis of the influences of beam parameters on the autoresonance extraction process. Section IV provides the conclusion.

II. THEORETICAL ANALYSIS AND SIMULATION

In nonlinear oscillator physical systems, the oscillation frequency depends on the oscillation amplitude, which is commonly referred to as detuning. To effectively excite the amplitude of such systems, a proven excitation technique called autoresonance can be used. Autoresonance is a phenomenon in nonlinear oscillators where the system automatically adjusts its amplitude in response to changes in the excitation frequency. Theoretically, the threshold of the autoresonance excitation is related to the detuning parameter of the system and the frequency sweep rate of the driver [15].

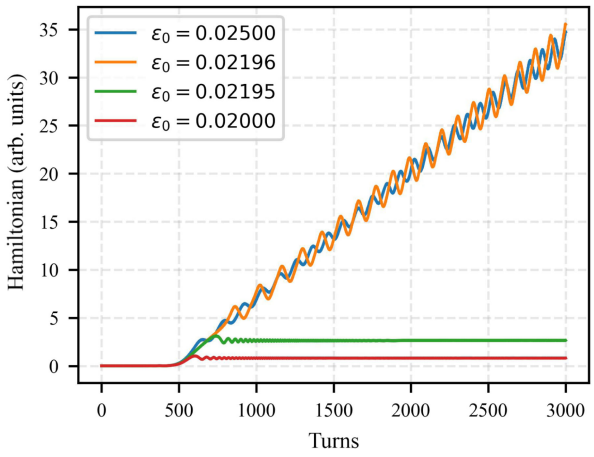


FIG. 1. Response of the oscillator with nonlinear detuning under different excitation amplitude.

As an illustrative example, all quantities in this example are given in arbitrary units. We assume a simple oscillator $x = A\cos(\omega_o t + \phi_o)$ oscillating under an excitation $\varepsilon = \varepsilon_0 \cos(\omega_d t + \phi_d)$, where the oscillation frequency is linearly related to the system Hamiltonian $\omega_o = \omega_{o0} + k_1 H$ and $H = (\omega_o^2 x^2 + x'^2)/2$, and the excitation frequency varies linearly with time $\omega_d = \omega_{d0} + k_2 t$. Figure 1 shows the response of the oscillator under different drive strengths with a time step of turns and $\omega_{o0} = 1.060$, $\omega_{d0} = 0.94 \times \omega_{o0} = 0.996$, $k_1 = 0.01$, and $k_2 = 1.33 \times 10^{-4}$. As shown in the figure, this oscillator has a very sharp threshold close to $\varepsilon = 0.02196$. When the excitation amplitude is above this threshold, autoresonance happens, as illustrated by the orange and blue curves in Fig. 1. Throughout the excitation process, the oscillation amplitude keeps increasing. Conversely, as shown by the red and green lines, the oscillation amplitude becomes nearly constant starting from a certain time, indicating that autoresonance is not achieved.

In recent years, the ultrahigh dose rate (FLASH) radiotherapy has become a novel cancer treatment technique because of its similar tumor-killing efficacy as conventional particle therapy while significantly protecting normal tissues. However, due to the limitation of the number of particles, achieving FLASH condition in a compact heavy-ion synchrotron requires a spill time of tens of milliseconds, which is challenging for the widely used rf-KO.

Conventional slow extraction rf-KO employs a repetitive multicycle frequency sweeping excitation, where a specific particle resonates when the sweeping frequency aligns with its tune. However, the extremely high dose rates required for FLASH therapy necessitate large excitation amplitudes that current rf technologies cannot adequately provide

within the required millisecond scale. By utilizing the autoresonance excitation mode, the required excitation amplitude can be reduced, allowing for the achievement of FLASH therapy requirements with lower excitation amplitude. To address this challenge, this paper introduces autoresonance into resonant extraction for the first time. By incorporating a strong detuning effect, this method increases particle oscillation amplitudes by phase locking using a single-cycle frequency sweeping excitation.

Leveraging the principles of autoresonance, this technique achieves whole beam amplitude resonance by phase-locking excitation, facilitating rapid and uniform beam extraction. Compared to conventional slow extraction methods, this innovative approach only requires the addition of an octupole magnet. Simulation results confirm the theoretical analysis, validating the effectiveness of the proposed autoresonance rapid extraction method.

A. Autoresonance threshold analysis

In this section, we present an analytical study of the autoresonance threshold in the presence of sextupole and octupole magnetic fields. The Hill's equation of particles in the horizontal direction under an excitation can be simply described by

$$x'' + K_1(s)x + \frac{K_2(s)}{2}x^2 + \frac{K_3(s)}{6}x^3 = \varepsilon \cos\phi_d \sum_n \delta(s - nC), \tag{1}$$

where $K_1(s)$, $K_2(s)$, $K_3(s)$ represent the horizontal focusing function of the quadrupole, sextupole, and octupole in the longitudinal coordinate s, the excitation is regarded as a δ function per revolution with an amplitude of ε, n is the number of turns, and C is the synchrotron circumference. The drive phase $\phi_{d,n} = 2\pi\nu_{d,n} + \phi_{d,n-1}$ depends on the drive phase $\nu_{d,n} = \nu_{d,0} + \alpha n$, where α is the tune sweeping rate and $\phi_{d,n-1}$ the initial phase for each turn. A more general form of the drive phase is $\phi_{d,n} = 2\pi(\nu_{d,0} + \frac{n+1}{2}\alpha)n + \phi_{d,0}$. After performing Floquet transformation and canonical transformation, the phase-space coordinate (x, x') can be transformed into action-angle space coordinate (J_x, Φ_x), and the position variable s turns to the azimuth $\theta = 2\pi s/C$. The new Hamiltonian for Eq. (1) expressed in action-angle variables with θ can be written as

$$H(J_x, \Phi_x; \theta) = \nu_x J_x + \frac{1}{2}\alpha_{xx}J_x^2 + \frac{\sqrt{2\beta_x J_x}}{4\pi}\varepsilon \cos(\Phi_x - \nu_d\theta) + V_3 + V_4, \tag{2}$$

where β_x is the beta function at the location of the excitation, $\nu_d(\theta) = \nu_{d0} + \frac{\theta+2\pi}{4\pi}\alpha = \nu_0 + \frac{\alpha}{4\pi}\theta$ is the effective excitation tune. For simplicity, we only consider the first-order nonlinear detuning effect of sextupole and octupole $\alpha_{xx} = \alpha_{xx,s} + \alpha_{xx,o}$. The discrete drive is expanded in a Fourier series, and here we only consider the lowest order term. V_3 and V_4 represent the third-order and fourth-order resonance terms that are caused by sextupole and octupole, respectively. For beam extraction, the betatron tune is close to 1/3, so that the fourth-order resonances can be ignored, and the third-order resonance driving term can be approximated by $V_3 = G_{3,0,l}J_x^{3/2}\cos(3\Phi_x - l\theta + \xi_{3,0,l})$. The resonance strength $G_{3,0,l}$ can be numerically calculated based on the synchrotron optics [20]. We assume that the excitation tune sweeps slowly around the extraction tune, i.e., $3\nu_d \approx l$, and perform again the canonical transformation by using the generating function $F_2 = \Psi_x J_x = (\Phi_x - \nu_d\theta)J_x$, the new Hamiltonian becomes

$$\hat{H}(J_x, \Psi_x; \theta) = (\nu_x - \nu_d)J_x + \frac{1}{2}\alpha_{xx}J_x^2 + k_0 J_x^{1/2}\cos\Psi_x + G_{3,0,l}J_x^{3/2}\cos 3\Psi_x, \tag{3}$$

where $k_0 = \frac{\sqrt{2\beta_x}}{4\pi}\varepsilon$. Now, the particle motion can be described by

$$\frac{dJ_x}{d\theta} = k_0 J_x^{1/2}\sin\Psi_x + 3G_{3,0,l}J_x^{3/2}\sin 3\Psi_x$$
$$\frac{d\Psi_x}{d\theta} = \nu_x - \left(\nu_0 + \frac{\alpha}{2\pi}\theta\right) + \alpha_{xx}J_x + \frac{1}{2}k_0 J_x^{-1/2}\cos\Psi_x + \frac{3}{2}G_{3,0,l}J_{x0}^{1/2}\cos 3\Psi_x. \tag{4}$$

Basically, it can be seen from Eq. (4) that when the excitation is off ($\varepsilon = 0$) and the third-order resonance strength is small, the particle action will remain constant and the phase will advance steadily. When the excitation driver is turned on, the action will increase or decrease depending on the phase, which is also affected by the value of the action J_x itself. Generally speaking, for a small action, the drive is primarily responsible for the phase changing, and correspondingly resulting in smooth changing of the action. When the action is large, it is difficult for the drive to change the phase and a strong phase mismatch will occur, causing the action to stop changing. This is similar to the conclusion about the pendulum in Refs. [14,15].

However, the phase actually depends on the drive strength k_0, frequency sweep rate α, detuning parameter of the machine α_{xx}, as well as the action value J_x. The occurrence of autoresonance exactly means that the system is phase locked and the action response always remains in phase with the drive, so that Ψ_x must remain near a constant. Therefore, we can analyze the threshold for the autoresonance based on the condition of phase lock. We assume that $G_{3,0,l}$ is small for particles with small action and far from the resonance. Then, the phase Ψ_x can be approximated as being locked around π and the action

varies smoothly with a small deviation $J_x = J_{x0} + \Delta$, where the equilibrium action J_{x0} can be obtained by

$$\nu_x - \left(\nu_0 + \frac{\alpha}{2\pi}\theta\right) + \alpha_{xx}J_{x0} - \frac{k_0}{2}J_{x0}^{-1/2} - \frac{3}{2}G_{3,0,l}J_{x0}^{1/2} = 0. \tag{5}$$

Substitute Eq. (5) into Eq. (4) and apply the first-order Taylor expansion of $J_x^{1/2}$ and $J_x^{-1/2}$, we get

$$\begin{aligned}\frac{d\Delta}{d\theta} &= k_0 J_{x0}^{1/2}\sin\Psi_x - \frac{\alpha}{2\pi S} + 3G_{3,0,l}J_{x0}^{3/2}\sin 3\Psi_x \\ \frac{d\Psi_x}{d\theta} &= S\Delta,\end{aligned} \tag{6}$$

where $S = \alpha_{xx} + \frac{1}{4}k_0 J_{x0}^{-3/2} - \frac{3}{4}G_{3,0,l}J_{x0}^{-1/2}$. So the Hamiltonian for the new canonical coordinates (Δ, Ψ_x) is

$$\begin{aligned}\tilde{H}(\Delta,\Psi_x;\theta) = \frac{1}{2}S\Delta^2 + k_0 J_{x0}^{1/2}\cos\Psi_x \\ + \frac{\alpha}{2\pi S}\Psi_x + G_{3,0,l}J_{x0}^{3/2}\cos 3\Psi_x.\end{aligned} \tag{7}$$

Now, the system reduces to a pseudoparticle of slowly varying effective mass $1/S$ moving in a slowly varying pseudopotential $V_{\text{pseudo}} = k_0 J_{x0}^{1/2}\cos\Psi_x + \frac{\alpha}{2\pi S}\Psi_x + G_{3,0,l}J_{x0}^{3/2}\cos 3\Psi_x$, which is cosine wave with a certain slope. For an autoresonance system that is phase locked, there must be a potential well in which the pseudoparticle is trapped and the phase mismatch is kept close to zero. We still assume the phase locked at $\Psi_x = \pi$, and the condition for the existence of this potential well is simple, i.e.,

$$\left|\frac{\alpha}{2\pi S}\right| < k_0 J_{x0}^{1/2} + G_{3,0,l}J_{x0}^{3/2}. \tag{8}$$

Based on the action of a particle and the setting parameters of the machine, the excitation condition that can drive the particle to autoresonance can be obtained by solving Eq. (8).

Theoretically, the autoresonance threshold is related to J_x, but so far, we have only observed this phenomenon in our simulation. To simplify the derivation process, we made approximations in our formulas, neglecting the effects of higher-order terms, among which the contribution from J_x is included. This specific derivation of the formulas and further simulations will be the focus of our future research. When only octupoles are involved, it can be found that there is a critical action $J_{x0} = (\frac{k_0}{2\alpha_{xx}})^{2/3}$ corresponding to the most difficult situation to achieve autoresonance. Substitute this into Eq. (8), the excitation threshold turns to $\varepsilon > 4\sqrt{2}\pi(\beta\alpha_{xx})^{-\frac{1}{2}}(\frac{\alpha}{6\pi})^{\frac{3}{4}}$. This is consistent with the result in Ref. [19]. With the sweep rate remaining unchanged, the larger the absolute value of α_{xx}, the smaller the threshold required to achieve autoresonance. Similarly, the autoresonance threshold in the presence of sextupole and octupole can be obtained by using this critical action $J_{x0} = (\frac{k_0}{2\alpha_{xx}})^{2/3}$:

$$-\frac{9\sqrt{2}}{8}G_{3,0,l}\sqrt{\beta_x}\varepsilon + \frac{3}{4(2\pi)^{1/3}}\alpha_{xx}^{\frac{2}{3}}(\sqrt{\beta_x}\varepsilon)^{\frac{4}{3}} > \alpha. \tag{9}$$

Under the condition that both $G_{3,0,l}$ and J_{x0} are relatively small, this approximation is reasonable.

In the above, the excitation conditions of autoresonance under the influence of sextupole and octupole magnetic fields are studied, which will provide theoretical guidance for the application of autoresonance in rapid beam extraction in synchrotrons. However, some approximations, such as the low-order Fourier approximation of the δ function and the small third-order resonance strength, may make the theoretical analysis less than perfect. Since we only focus on exciting the beam with small emittance in the stable region to a large amplitude, thereby realizing the beam extraction in the nonlinear region, the assumption that the third-order resonance strength is small in the above derivation is reasonable. For large-amplitude particles close to the resonance line, the effect of the sextupole on the resonance strength and the detuning parameter will strongly affect the autoresonance condition, for which the above derivation may not be well applicable. Regardless, a numerical simulation is very necessary for benchmarking with the theory and for more efficient analysis of the autoresonance threshold.

B. Single particle simulation

To verify the theory presented in Sec. II A, a single particle simulation is performed based on the slow extraction lattice of SESRI synchrotron at Harbin Space Environment Simulation Research Infrastructure [9]. The lattice of the synchrotron is shown in Fig. 2, and the major parameters are listed in Table I. We use the multiparticle tracking code SESP, which is based on the linear transfer matrix, with nonlinear elements treated using a thin-lens approximation. The code has been successfully applied to

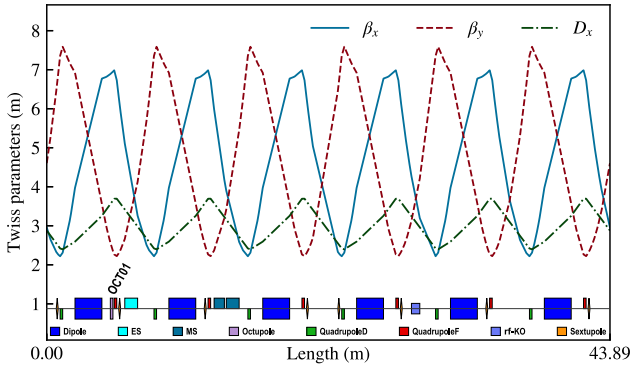


FIG. 2. Lattice of the SESRI synchrotron.

TABLE I. Major parameters of the synchrotron.

Circumference (m)	43.89
Ion species	p to $^{209}Bi^{32+}$
Maximal energy (MeV/u)	300(p), 7 ($^{209}Bi^{32+}$)
Beam intensity (ppp)	1×10^{9}(p), 1×10^{7}(Bi)
Magnetic rigidity (Tm)	0.34–2.80
Tune Q_x/Q_y	1.689/1.736
Emittance of extraction $\epsilon_h/\epsilon_v(\pi\,\mu m)$	26/4(p), 107/15($^{209}Bi^{32+}$)
Natural chromaticity ξ_x/ξ_y	−0.71/ − 1.03
Third-order resonance strength $G_{3,0,5}(m^{-1/2})$	0.00608
First-order detuning parameter caused by sextupoles (m^{-1})	−25.99
Octupole beta function (m)	$\beta_x/\beta_y = 6.89/2.57$
rf-KO beta function (m)	$\beta_x/\beta_y = 4.27/3.16$

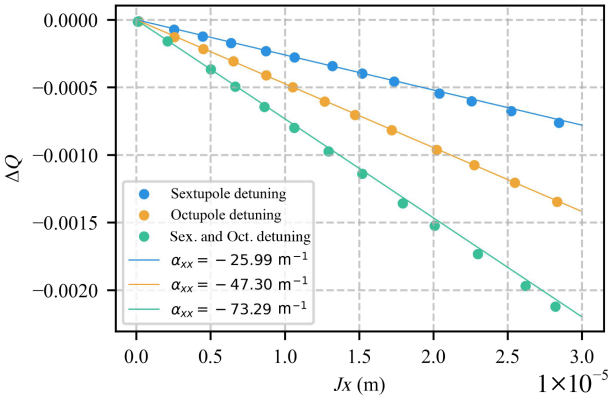


FIG. 3. Comparison of simulation and theoretical results for the tune shifts with only sextupole, only octupole, and both.

the design of the SESRI [21]. Our simulation employs the 7 MeV/u Bi beam.

There are eight sextupole magnets symmetrically distributed in the synchrotron. Based on the design, the theoretical strength of the third-order resonance $G_{3,0,5}$ is about 0.00608 $m^{-1/2}$, and the calculated first-order nonlinear detuning parameter $\alpha_{xx,s}$ is about −25.99 m^{-1}. In the simulation, an octupole is introduced to achieve strong detuning, thereby reducing the autoresonance threshold. Assuming the octupole length: $l = 0.2$ m and the coefficient: $K_3 = -250.5\ m^{-4}$, a detuning parameter $\alpha_{xx,o} = -47.30\ m^{-1}$ is obtained (costing approximately 28,000 dollars for the magnet and its power supply).

The octupole is located near a horizontal focusing quadrupole to minimize the effect of the nonlinear field on the vertical motion. The impact for the vertical direction tune under one octupole magnet is: $Q_y = \nu_y + \alpha_{yy}J_y + \alpha_{xy}J_x + \cdots$. The octupole magnet is positioned at locations with $\beta_x/\beta_y = 6.89/2.57$. Under the extraction emittance: $\epsilon_h/\epsilon_v \approx 7$, so $J_x/J_y \approx 7$. Both $\alpha_{yy} = 1/16\pi \oint \beta_y^2 K_3 ds$ and $\alpha_{xy} = (-1)/8\pi \oint \beta_x\beta_y K_3 ds$ are relatively small, leading to a low ΔQ_v value. Thus, the octupole magnet has minimal influence on the vertical direction.

The detuning parameters are calculated based on the betatron motion of particles with different actions, using the PyNAFF [22,23] code. As shown in Fig. 3, the dependence of the tune shift on the action under the presence of only sextupoles, only octupoles, and both is obtained. The tracking detuning parameters are consistent with the theoretical values. However, we do not consider the higher order detuning near the third-order resonance. This factor could be important for particles with large actions close to the extraction orbit.

In the simulation, a cosine wave driver with a unidirectional frequency sweep is employed. The frequency follows $f_d = f_s + (f_e - f_s)\frac{n}{N}$, where n is the current number of turns, and N is the total simulation number of turns. The frequency sweep rate is controlled by adjusting the total number of simulation turns. Starting from the base frequency, the excitation frequency is swept downward when the detuning parameter is positive, and upward in the opposite case. In our case, the base frequency is $f_s = 1.4103$ MHz, which is slightly above $\nu_x f_0$ to ensure coverage of all particles with different emittances, where ν_x is the linear betatron tune and $f_0 = 0.8328$ MHz is the revolution frequency. The final frequency $f_e = 1.3928$ MHz corresponds to the design extraction tune of 1.676.

The tracking results of the evolution of betatron tune and oscillation amplitude of a particle with small J_x under different excitation amplitudes are presented in Fig. 4. For the excitation amplitude of $\varepsilon_0 = 4.07$ μrad, the drive phase

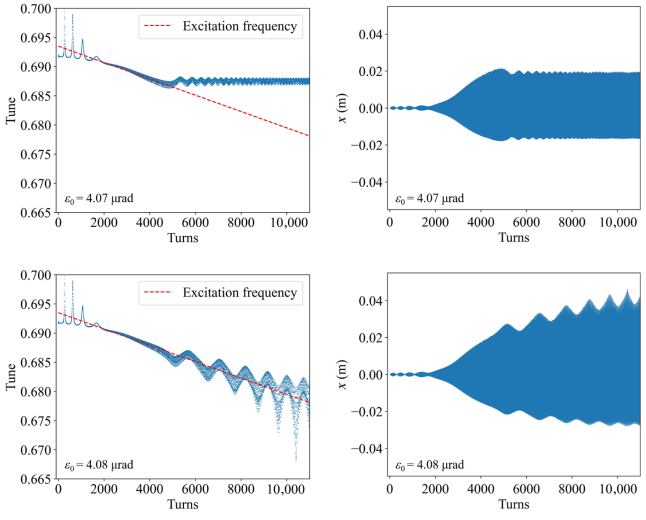


FIG. 4. Evolution of the single particle (initial emittance of $1\times10^{-5}\ \pi\,\mu m$) tune and betatron amplitude below (up) and above (down) the threshold, which is between 4.07 and 4.08 μrad.

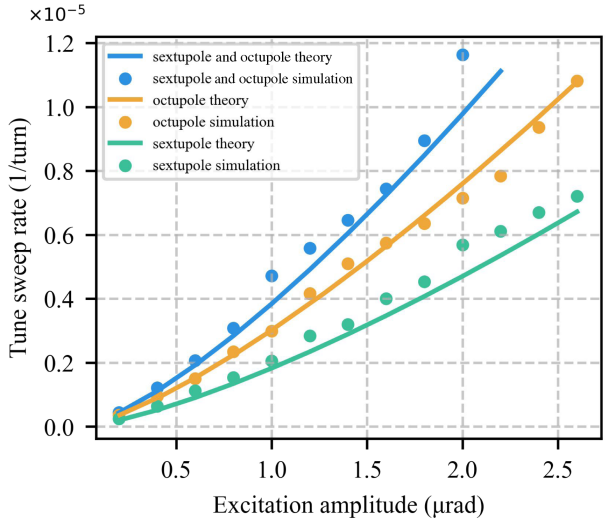


FIG. 5. Relationship between the autoresonance excitation threshold and the frequency sweep rate, which shows the simulation results are consistent with the theoretical calculations.

and the particle oscillation phase are mismatched after 5000 turns, so autoresonance is not excited. For the excitation amplitude of $\varepsilon_0 = 4.08$ μrad that is above the threshold, it results in a continuous increase of particle amplitude and phase lock between particle oscillation and the drive. It is clear that the autoresonance threshold is quite sharp and there is a significant difference in particle motion above and below the threshold.

Using the criterion of whether the phase is maintained locked throughout the entire simulation process, the autoresonance thresholds under different conditions are calculated. Figure 5 shows the relationship between the excitation threshold and the frequency sweep rate for the cases with only octupole, only sextupole, and both. The theoretical result Eq. (9) is consistent with those obtained from particle simulations. In particular, the result for the case with only an octupole agrees well with those presented in Ref. [19]. However, it is worth noting that the linear betatron tune we set is slightly away from one third, making the third-order resonance strength G small. This is consistent with the assumption introduced in Sec. II, so that the theoretical curves with sextupoles are in good agreement with the simulation.

It also demonstrates that the extra detuning introduced by the octupole can reduce the excitation threshold, thus achieving a more effective rapid extraction method than the conventional rf-KO slow extraction. Theoretically, the requirement of the excitation can be significantly reduced by a stronger detuning, as long as it does not strongly affect the extraction separatrix. In the subsequent section, the rapid extraction method based on the autoresonance will be introduced, and the differences and advantages over the conventional slow extraction will be discussed.

III. AUTORESONANCE-BASED RAPID EXTRACTION

In the conventional rf-KO slow extraction method, the tune needs to be adjusted to be close to the third-order resonance line using quadrupole magnets after acceleration. Conventional slow extraction rf-KO employs a repetitive multicycle frequency sweeping excitation, as shown by the blue curve in Fig. 6. Single-frequency or dual-frequency excitation with a sweep range of several hundred hertz is used to drive particle oscillation amplitude [10]. Once particles are outside the stable triangle in phase space, formed by the sextupoles, their motion tends toward the three separatrices. The particles follow separatrices into the extraction channel, resulting in successful extraction. Throughout this process, a small bunch of particles is excited and extracted during each excitation sweep cycle. As a result, the overall extraction spill structure displays multiple peaks.

In conventional rf-KO slow extraction, the excitation amplitude remains below the autoresonance threshold. Consequently, particles are excited only when the frequency sweep aligns with their transverse oscillation frequency during each sweep cycle. Over multiple excitation periods, as the frequency sweep range encompasses all particle tunes, the beam appears to undergo continuous extraction over several seconds. However, at a microscopic level, its spill structure reveals a periodic pattern dictated by the frequency sweep cycle, resulting in multiple distinct distributions [10].

Autoresonance rapid extraction employs single-cycle frequency sweeping excitation, as illustrated in Fig. 6, with a sweep range from $\nu_s f_0$ to $\nu_e f_0$, where ν_s is the linear tune, ν_e is the design extraction tune, and f_0 is revolution frequency. There is no need for specific adjustment of the accelerator's linear tune in the entire operation cycle. As the amplitude increases, the tune of particles automatically moves toward the resonance line due to the detuning effect

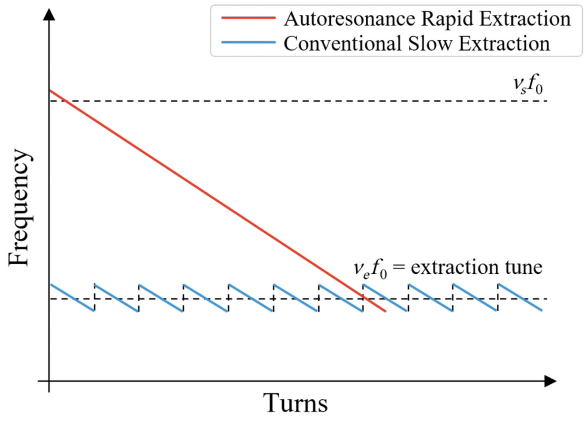


FIG. 6. Schematic comparing the autoresonance rapid extraction frequency sweeping curve (red) and conventional slow extraction single-frequency sweeping curve (blue).

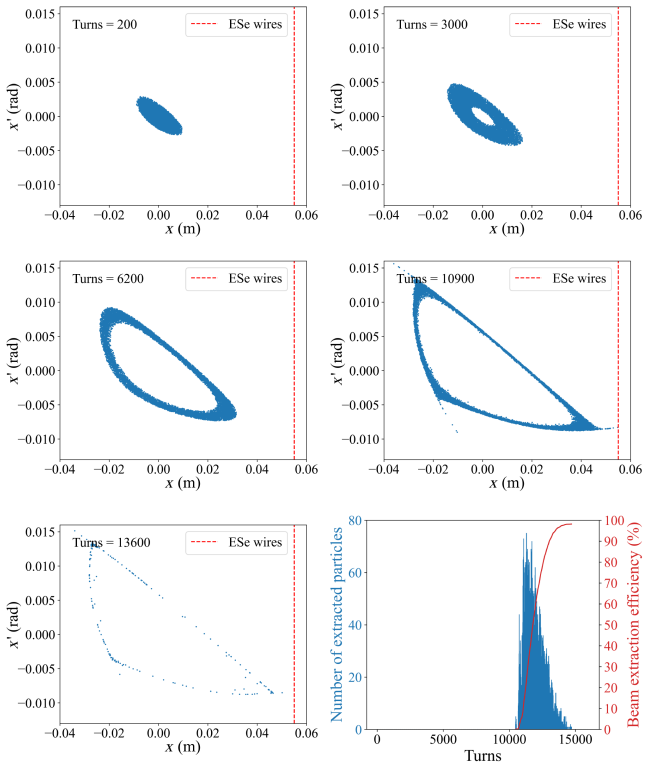


FIG. 7. Simulation results of the beam distribution in phase space during the process of the autoresonance-based rapid extraction. The excitation amplitude is 10 μrad and the frequency sweep rate is 1.4×10^{-6}. The location of ESe wires is indicated by the red dashed line.

caused by the octupole and sextupole magnets. The single-cycle frequency sweeping excitation causes the oscillation amplitudes of all particles to increase collectively, as shown in Fig. 7, and this results in only one peak in the spill structure.

In contrast, autoresonance rapid extraction method utilizes strong detuning to reduce the autoresonance threshold. During this process, all particles in the beam are strongly excited within a single-cycle frequency sweeping excitation, reducing the spill time to the millisecond scale. The spill structure of this method exhibits a single Rayleigh distribution like the bottom right figure in Fig. 7, but the desired uniform distribution can be achieved through standard techniques such as preset excitation amplitude modulation and real-time feedback system. Additionally, the strong detuning requires the initial tune to be set further away from the third-order resonance line, which is beneficial for the beam's stability.

To compare the number of turns required for conventional slow extraction and autoresonance rapid extraction, we conducted simulations using a multiparticle approach with parameters consistent with those in the previous section. The excitation amplitude was set at discrete values from 5 to 50 μrad in 5 μrad increments. For autoresonance rapid extraction method with an

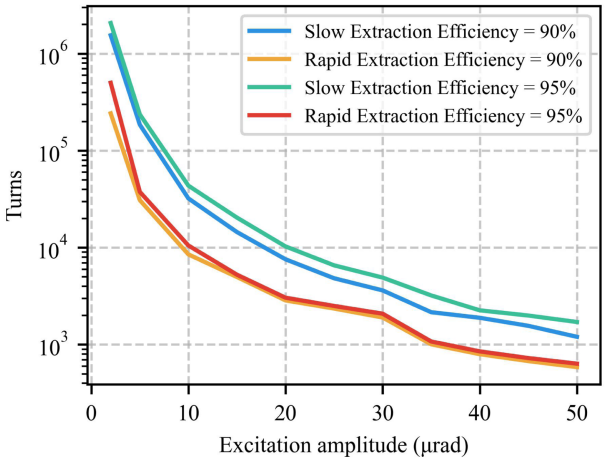


FIG. 8. Comparison of the number of turns required for conventional slow extraction and autoresonance rapid extraction for different extraction efficiencies.

octupole, the frequency sweep of the simulation ranged from $\nu_s f_0 = 1.690 \times 0.8328 \times 10^6$ Hz to $\nu_e f_0 = 1.675 \times 0.8328 \times 10^6$ Hz, and the sweep rate was modulated by adjusting the total number of simulation turns N, with the sweep rate being inversely proportional to N. In contrast, the conventional slow extraction method without the octupole used a fixed sweep rate, with a frequency sweep period of $1/200$ Hz $= 5$ ms and the sweep range from 1395517.97 to 1395017.97 Hz. For each excitation amplitude, we recorded the minimum number of turns required to achieve the same extraction efficiency (defined as the ratio of extracted particles to the total simulated particle population).

The comparison results are shown in Fig. 8. The results indicate that the extraction time of autoresonance rapid extraction is nearly an order of magnitude shorter than that of conventional slow extraction. Furthermore, the spill time in autoresonance rapid extraction accounts for only a small fraction of the total extraction time. In contrast, conventional slow extraction requires time for tune adjustment and has beam spill time spanning almost the entire process, making autoresonance rapid extraction more effective at achieving short spill times. On the other hand, Fig. 8 shows that to achieve the same total number of turns for extraction, the required excitation amplitude for conventional slow extraction is approximately twice that of autoresonance rapid extraction. Achieving a 10 ms extraction time by upgrading the rf-KO system for conventional rf-KO extraction incurs costs that are approximately 3 to 5 times greater than the cost of the octupole and its power supply, as mentioned above.

A. The influence of beam initial emittance and momentum spread

In the previous section, we found that autoresonance is related to certain beam parameters. Therefore, we

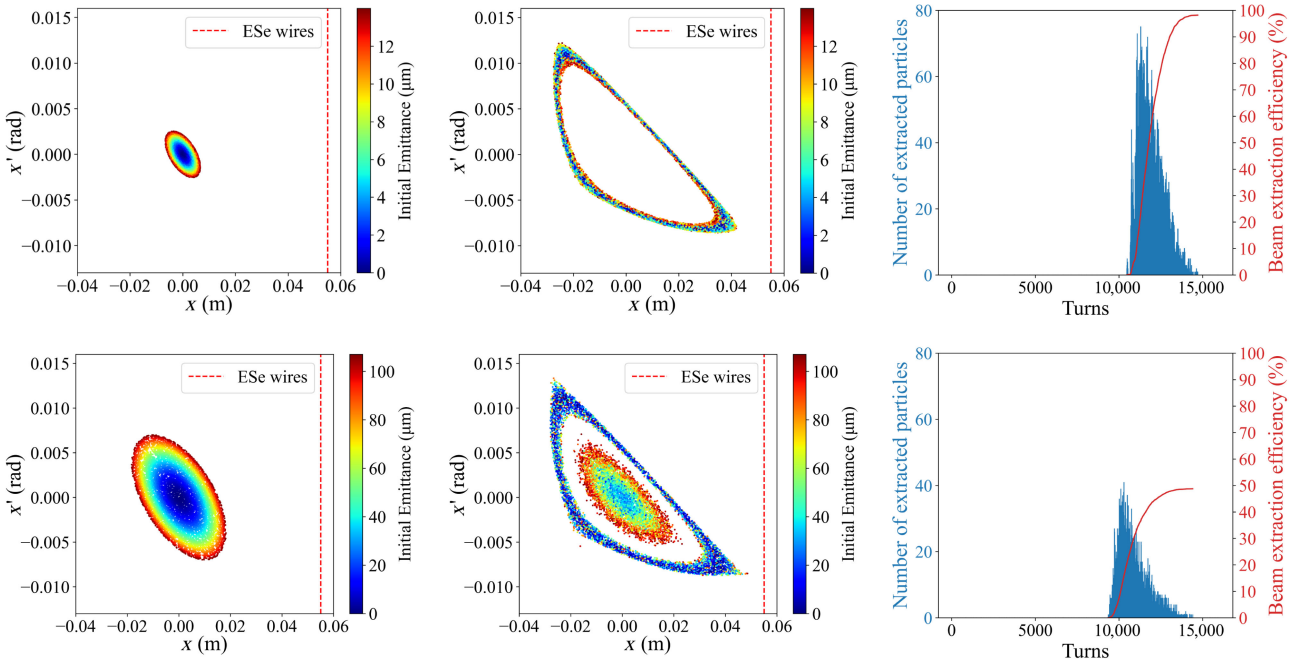


FIG. 9. Comparison of the simulated beam distribution in phase space and the spill structure for different beam initial emittances (top: 14 π μm; bottom: 107 π μm). The first column shows the initial beam distribution; the second column shows the horizontal phase space distribution at the beginning of extraction (9400th turn); the third column shows the spill structure and extraction efficiency.

conducted a study to examine the relationship between autoresonance and initial emittance, as well as the relationship between autoresonance and momentum spread.

To investigate the effect of the beam emittance on autoresonance excitation, simulations are conducted in the SESRI synchrotron for beams with different initial emittance and zero momentum spread. The excitation amplitude is set to 10 μrad, and tracking is performed over 15,000 turns.

The top left figure in Fig. 9 shows the initial distribution of the simulated beam with the initial emittance of 14 π μm. With this initial emittance, during the simulation process, all particles' amplitudes are simultaneously excited. The beam forms a distinct beam halo in phase space, as shown in the top middle figure in Fig. 9, indicating that the entire beam achieves autoresonance. Beam extraction begins around the 10,500th turn, and by the 15,000th turn, the extraction efficiency reaches 98.2%.

The bottom left figure in Fig. 9 shows the initial distribution of the simulated beam with the initial emittance of 107 π μm. With this initial emittance, some particles' oscillation amplitudes stop increasing after a certain period. Subsequently, the particles in the "blue beam halo" will be extracted. What happens during one frequency sweep period in conventional slow extraction is quite similar to this situation, where a part of the particles is extracted with each sweep period [24]. As shown in the bottom middle figure of Fig. 9, which represents the simulation of beams with larger initial emittance. Simulation results show that beams with larger emittance require a larger excitation amplitude to achieve autoresonance. By the 15,000th turn, the beam extraction efficiency is only 48.8%. To improve the extraction efficiency, one solution is to deepen the potential well by either increasing the excitation amplitude or adjusting the detuning parameter as Eq. (9). This approach makes it possible for particles that are challenging to excite to larger amplitudes to resonate and be successfully extracted. Both initial emittance conditions' spill structure exhibits a Rayleigh distribution, consistent with the beam spill structure observed in one of the periods during the conventional slow extraction process.

Figure 10 illustrates the dependence of the excitation threshold on beam emittance through simulation results. By tracking 10,000 particles, we aim to bring at least 99.7% of them into autoresonance and record the minimum excitation threshold required with initial emittance ranging from 10 to 100 π μm. The results further validate the findings in Fig. 9, demonstrating that particles with larger initial emittance are more difficult to achieve autoresonance, thus requiring a higher amplitude.

In addition, to investigate the effect of the momentum spread on autoresonance excitation, simulations with momentum spreads of 0.1% and 0.5% are conducted as shown in Fig. 11. The emittance in this simulation is set to 14 π μm, and the excitation amplitude is set to 10 μrad. Due to the existence of a 3.4 m dispersion at the observation point, the "beam halo" formed by the beam with a larger momentum spread has a wider width. Consequently, this

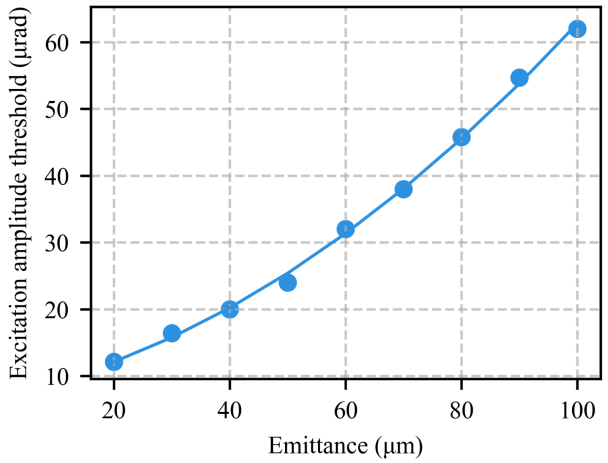


FIG. 10. Simulation results of the dependence of the excitation threshold on the beam emittance.

leads to a phenomenon where the extraction structure becomes broadened. The chromaticity within the synchrotron is $\xi_x/\xi_y = -0.71/-1.03$, which should bring a maximum tune shift of 0.005. The simulation shows that momentum spread has little effect on autoresonance. As long as the frequency sweep can cover the corresponding range, a larger momentum spread beam can still achieve autoresonance. The simulation results indicate that neither autoresonance excitation nor conventional rf-KO excitation will disrupt the third-order resonance slow extraction process.

We have also conducted simulations on the octupole effect on the separatrix. The octupole magnet introduces nonlinear perturbations that can bend the separatrix. Figure 12 shows the octupole effect on the separatrix. The red points represent the extraction phase space of conventional slow extraction without octupole fields. The blue points represent the extraction phase space of autoresonance rapid extraction with an octupole of strength: $K_3 = -250.5\ \mathrm{m}^{-4}$. Although there are differences between these two separatrices, they have almost no impact on the extraction efficiency when the strength of the octupole magnet is relatively low, as in our simulation. However, if the strength of the octupole magnets is relatively strong, the separatrix will bend more, necessitating a redesign of the extraction parameters to achieve better extraction performance.

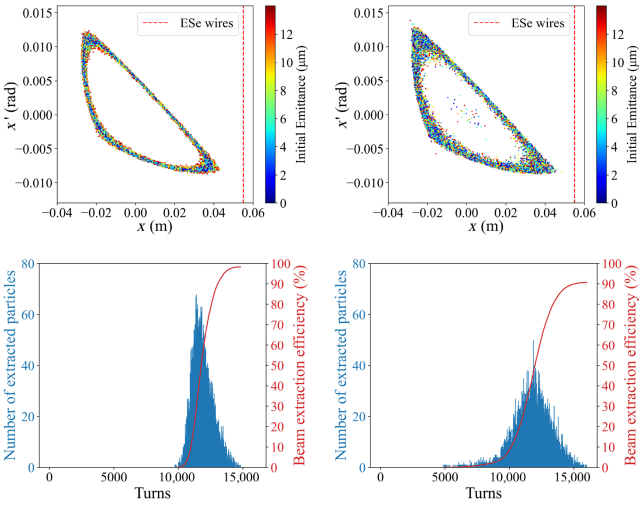


FIG. 11. Comparison of the simulated beam distribution in phase space and the extracted structure under different momentum spreads (left: $dp/p = 0.1\%$; right: $dp/p = 0.5\%$).

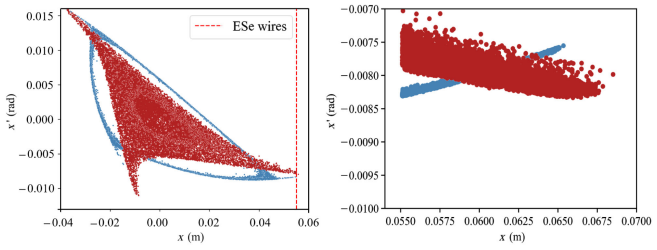


FIG. 12. Left figure is comparison of the beam distributions during extraction between slow extraction (red) and autoresonance rapid extraction (blue). Right figure is comparison of the beam distributions at electrostatic septum between slow extraction (red) and autoresonance rapid extraction (blue).

The right figure in Fig. 12 shows the conventional slow extraction and autoresonance rapid extraction distributions at electrostatic septum. The blue points show that, for autoresonance rapid extraction, both the maximum spiral step and the angular spread are within the design range.

B. Autoresonance rapid extraction advantage

Compared to conventional slow extraction, autoresonance rapid extraction exhibits several notable differences. First, particles in autoresonance state are characterized by a phase locking of their oscillation frequency to the excitation frequency, allowing for strong excitation of particle amplitude with a smaller excitation amplitude or facilitating a reduction in spill time to the millisecond range. Second, autoresonance rapid extraction requires strong detuning, requiring that the initial tune be far away from the third-order resonance line, which provides additional stability for the beam. Additionally, autoresonance rapid extraction eliminates the need for quadrupole magnets to modify the tuning, thereby simplifying the extraction process and potentially further reducing the extraction time. Third, during the amplitude excitation process in autoresonance rapid extraction, the detuning is primarily governed by the action in phase space, which corresponds to the particle's amplitude. The detuning is solely determined by the parameters of the nonlinear magnets in phase space. Consequently, precise control over the particle's amplitude can be achieved by merely adjusting the nonlinear magnets and the driver.

IV. CONCLUSION

The autoresonance technique enables nonlinear oscillators to achieve large oscillation amplitudes by applying a swept frequency excitation, where the beam remains phase locked with the drive once the excitation amplitude is above a specific threshold. In this study, we derived the autoresonance threshold for an oscillator under the influence of sextupole and octupole magnetic fields, with single particle simulations showing good agreement with the theoretical formula. Benefiting from the strong detuning effect introduced by octupole, autoresonance can be efficiently driven by an excitation with small amplitude. Accordingly, we propose a rapid beam extraction method for synchrotrons and demonstrate its feasibility through theoretical analysis and simulation.

In the proposed rapid extraction, the entire beam is brought into autoresonance by aligning the excitation amplitude with the threshold conditions. As the oscillation amplitude increases and approaches the third-order resonance, the separatrix dominated by sextupole field enables the particle to enter the extraction channel. This allows for beam extraction within one sweeping period on the order of millisecond. Simulations on SESRI synchrotron validate the theoretical framework and confirm the capability of millisecond slow extraction requirement for FLASH radiotherapy using existing excitation techniques. Compared with the conventional rf-KO method, this innovative method requires only the addition of one octupole magnet, and the power requirement of the driver can be significantly reduced, thus mitigating potential risks associated with high-power drives. Concurrently, this method eliminates the need for tune adjustment also simplifies operational complexity and may further reduce the proportion of the extraction platform throughout the entire operation cycle.

Our findings suggest that autoresonance offers a promising solution to the challenges of rapid beam extraction in synchrotrons, providing a more efficient and safer operational pathway for both medical applications and high-energy physics research. Future efforts will concentrate on the experimental implementation of this technique in an operational synchrotron, as well as on further optimization of parameters for extraction efficiency and beam quality.

ACKNOWLEDGMENTS

The authors would like to thank colleagues in the accelerator physics group at IMP for useful suggestions and discussions. Thanks to G. Y. Zhu for the discussion on the excitation system. This work is supported by the National Natural Science Foundation of China (Grants No. 12425501, No. 12275323, No. 12405177), the Hundred Talents Project of the Chinese Academy of Sciences, the Natural Science Foundation of Gansu Province, China (Grant No. 25JRRA459), and the Gansu Intellectual Property Plan (Grant No. 24ZSCQD002).

DATA AVAILABILITY

The data that support the findings of this article are openly available [25].

[1] W. Tinganelli, O. Sokol, M. Quartieri, A. Puspitasari, I. Dokic, A. Abdollahi, M. Durante, T. Haberer, J. Debus, D. Boscolo, B. Voss, S. Brons, C. Schuy, F. Horst, and U. Weber, Ultra-high dose rate (FLASH) carbon ion irradiation: Dosimetry and first cell experiments, Int. J. Radiat. Oncol. Biol. Phys. **112**, 1012 (2022).

[2] PTCOG-patient statistics, 2024, https://www.ptcog.site/index.php/patient-statistics-2.

[3] J. C. L. Chow and H. E. Ruda, Mechanisms of action in FLASH radiotherapy: A comprehensive review of physicochemical and biological processes on cancerous and normal cells, Cells **13**, 835 (2024).

[4] P. G. Maxim, P. Keall, and J. Cai, FLASH radiotherapy: Newsflash or flash in the pan?, Med. Phys. **46**, 4287 (2019).

[5] S. Jolly, H. Owen, M. Schippers, and C. Welsch, Technical challenges for FLASH proton therapy, Phys. Med. **78**, 71 (2020).

[6] N. W. Colangelo and E. I. Azzam, The importance and clinical implications of FLASH ultra-high dose-rate studies for proton and heavy ion radiotherapy, Radiat. Res. **193**, 1 (2019).

[7] L. Badano, M. Crescenti, P. Holy, A. Maier, P. Knaus, P. Bryant, M. Benedikt, M. Pullia, and S. Rossi, Proton-ion medical machine study (PIMMS), 1, Technical Report No. CERN-PS-99-010-DI, CERN, European Organization for Nuclear Research, Supported by Med-AUSTRON, Onkologie-2000, and TERA Foundation, 1999.

[8] K. Noda, T. Furukawa, S. Shibuya, M. Muramatsu, T. Uesugi, M. Kanazawa, M. Torikoshi, E. Takada, and S. Yamada, Source of spill ripple in the rf-KO slow-extraction method with FM and AM, Nucl. Instrum. Methods Phys. Res., Sect. A **492**, 241 (2002).

[9] S. Ruan, J. C. Yang, J. W. Xia, Y. J. Zheng, R. L. Wang, X. J. Yin, G. D. Shen, L. N. Sheng, C. Qian, G. Wang, W. P. Chai, J. Liu, F. C. Cai, Y. P. Yao, and L. X. Hou, The 300 MeV proton and heavy ion accelerator complex for SESRI project in china, Nucl. Instrum. Methods Phys. Res., Sect. A **1048**, 167916 (2023).

[10] K. Noda, T. Furukawa, S. Shibuya, T. Uesugi, M. Muramatsu, M. Kanazawa, E. Takada, and S. Yamada, Advanced rf-KO slow-extraction method for the reduction of spill ripple, Nucl. Instrum. Methods Phys. Res., Sect. A **492**, 253 (2002).

[11] B. Meerson and L. Friedland, Strong autoresonance excitation of Rydberg atoms: The Rydberg accelerator, Phys. Rev. A **41**, 5233 (1990).

[12] W.-K. Liu, B. Wu, and J.-M. Yuan, Nonlinear dynamics of chirped pulse excitation and dissociation of diatomic molecules, Phys. Rev. Lett. **75**, 1292 (1995).

[13] J. Fajans, E. Gilson, and L. Friedland, Autoresonant (nonstationary) excitation of the diocotron mode in non-neutral plasmas, Phys. Rev. Lett. **82**, 4444 (1999).

[14] J. Fajans, E. Gilson, and L. Friedland, Autoresonant (nonstationary) excitation of a collective nonlinear mode, Phys. Plasmas **6**, 4497 (1999).
[15] J. Fajans and L. Frièdland, Autoresonant (nonstationary) excitation of pendulums, plutinos, plasmas, and other nonlinear oscillators, Am. J. Phys. **69**, 1096 (2001).
[16] L. Friedland, Control of Kirchhoff vortices by a resonant strain, Phys. Rev. E **59**, 4106 (1999).
[17] G. Klughertz, L. Friedland, P.-A. Hervieux, and G. Manfredi, Autoresonant switching of the magnetization in single-domain nanoparticles: Two-level theory, Phys. Rev. B **91**, 104433 (2015).
[18] A. Shagalov and L. Friedland, Narrow autoresonant magnetization structures in finite-length ferromagnetic nanoparticles, Phys. Rev. E **100**, 032208 (2019).
[19] M. Song, L. Spentzouris, X. Huang, and J. Safranek, Autoresonant excitation of nonlinear beam motion in storage rings, Phys. Rev. Accel. Beams **25**, 074001 (2022).
[20] S.-Y. Lee, *Accelerator Physics* (World Scientific, Singapore, 2018).
[21] Y. Z. Gao, S. Ruan, J. Shi, J. C. Yang, J. W. Xia, Y. Li, and Y. Zhou, Study on slow extraction dynamics of 300 MeV proton and heavy ion synchrotron, Nucl. Phys. Rev. **40**, 207 (2023).
[22] J. Laskar, The chaotic motion of the solar system: A numerical estimate of the size of the chaotic zones, Icarus **88**, 266 (1990).
[23] N. K. Panos Zisopoulos, A Python module that implements the numerical analysis of fundamental frequencies (NAFF) algorithm, 2023, https://pypi.org/project/pynaff/.
[24] E. Cortés García, P. Niedermayer, R. Singh, R. Taylor, E. Feldmeier, M. Hun, E. Benedetto, and T. Haberer, Interpretation of the horizontal beam response near the third integer resonance, Phys. Rev. Accel. Beams **27**, 124001 (2024).
[25] X. Ding, Application of autoresonance in rapid beam extraction of synchrotrons dataset, Zenodo, 10.5281/zenodo.14961642.